A New Dynamic Energy Stability Margin for Walking Machines

E. Garcia

Automatic Control Department
Industrial Automation Institute
La Poveda, 28500 Madrid, Spain
egarcia@iai.csic.es

P. Gonzalez de Santos

Automatic Control Department
Industrial Automation Institute
La Poveda, 28500 Madrid, Spain
pgds@iai.csic.es

Abstract

Previous work on the classification of stability criteria for walking machines reveals that there is no stability margin that accurately predicts robot stability when inertial and manipulation effects are significant. The use of an improper stability criterion yields unavoidable errors in the control of walking robots. Moreover, inertial and manipulation effects usually appear in the motion of these robots when the machines are used for services or industrial applications. A new stability margin that accurately measures robot stability considering dynamic effects arising during motion is proposed in this paper. The new stability margin is the optimum from the energy point of view. Numerical comparison has been conducted to support the margin's suitability.

1 Introduction

Legged locomotion has advantages on uneven terrain that make walking machines especially suitable for industrial and non-industrial applications, such as terrestrial and planetary exploration and humanitarian de-mining. Walking robots that have been designed for industrial purposes perform statically stable gaits [8, 11]. However, if statically stable gaits are to be adopted, there must be no dynamic effects during motion, and thus these machines are limited to low, constant speeds to avoid inertial effects. Little effort has been made to cope with the dynamic effects that limit statically stable machines' performance [4, 7, 10].

Recent research on the qualitative classification of stability margins for walking robots performing statically stable gaits has shown that currently there is a lack of stability margins to measure robot stability accurately when inertial and manipulation effects become involved [1]. These are precisely the dynamic effects that usually exist during the motion of walking robots in real services and industrial applications. Therefore, the main goal of this paper is to propose a new stability criterion for statically stable gaits, whose stability margin accurately measures robot stability when inertial and manipulation effects exist. The proposed margin is an extension of the Energy Stability Margin, ESM [9] to the consideration of robot dynamics and therefore has been named **Normalized Dynamic Energy Stability Margin, NDESM**.

This paper is structured as follows: First, the Normalized Dynamic Energy Stability Margin is proposed in Section 2, and it is numerically compared with other stability margins in Section 3. Finally, Section 4 presents some conclusions.

2 Normalized Dynamic Energy Stability Margin

The optimum stability margin from the energy viewpoint is the one that quantifies the maximum impact energy that the machine can absorb without losing stability. Following this definition, the ESM (see Appendix A) is optimum under static conditions, e.g. when the only significant force acting on the robot is gravity, as previously demonstrated [5]. The ESM is computed from the increment of potential energy that the machine's center of gravity (CG) experiences when pivoting around the edges of the support polygon. Therefore, the extension of the ESM to the presence of other robot dynamics, like inertial forces or manipulation effects, must compute the increment of mechanical energy that the CG experiences during the tumble. This idea was proposed by Ghasempoor and Sepehri [2] to measure robot stability in the application to wheel-based mobile manipulators. In this

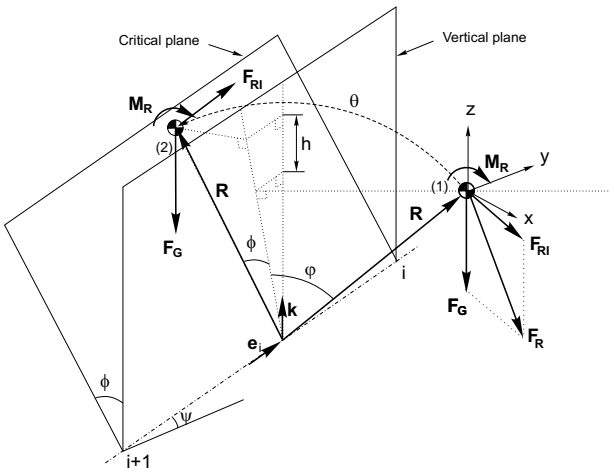

Figure 1: Geometric outline for the computation of the NDESM.

paper, Ghasempoor and Sepehri's idea has been extended to walking machines, considering leg dynamics as a destabilizing effect.

Let us consider a walking robot during its motion, where gravitational, inertial and manipulation forces and moments become significant. At a given instant an external perturbation causes the robot to tumble around one edge of its support polygon. Figure 1 depicts the CG of a robot during the tumble around the edge of its support polygon, given by the alignment of footprints i and $i+1$. This edge is inclined at an angle ψ from the horizontal plane due to terrain inclination. If the moment around this rotational axis caused by the resultant forces and moments of robot/ground interaction, $\mathbf{F_R}$ and $\mathbf{M_R}$, is able to compensate for the destabilizing effect, the robot could maintain stability. If, on the contrary, the effect cannot be compensated for, the robot will lose stability. Therefore, the instant of critical stability occurs when the moment of both robot/ground interaction forces and moments around the rotation axis vanishes. At that time the CG is located inside a **critical plane** that forms an angle ϕ with the vertical plane (see position (2) in Figure 1).

At the initial position (1) before the tumble, the CG is subject to inertial forces and moments ($\mathbf{F_I}$ and $\mathbf{M_I}$), gravitational forces and moments ($\mathbf{F_G}$ and $\mathbf{M_G}$), and manipulation forces and moments ($\mathbf{F_M}$ y $\mathbf{M_M}$). The perturbing effects of a leg in transfer phase can be also considered as manipulation terms. Assuming that the dynamics of the legs in the support phase is negligible relative to the body dynamics, the resultant force and moment of robot/ground interaction are given by:

$$\mathbf{F_R} = \mathbf{F_G} + \mathbf{F_M} - \mathbf{F_I} \tag{1}$$

$$\mathbf{M_R} = \mathbf{M_G} + \mathbf{M_M} - \mathbf{M_I} \tag{2}$$

During the tumble from position (1) to position (2), the gravitational force, $\mathbf{F_G}$, remains constant, while the rest of forces and moments rotate with the robot reference frame. Therefore let us divide the resultant robot/ground interaction forces, $\mathbf{F_R}$, into two components: one gravitational and the other non-gravitational. Let us name the non-gravitational component $\mathbf{F_{RI}}$, that is:

$$\mathbf{F_{RI}} = \mathbf{F_R} - \mathbf{F_G} \tag{3}$$

The mechanical energy increment experienced by the CG during the tumble from position (1) to position (2) is given by the following energy balance:

$$E_i = V_2 - V_1 + K_2 - K_1 \tag{4}$$

where V_1 and K_1 are the potential and kinetic energies of the CG respectively before the tumble (1), and V_2 and K_2 are the potential and kinetic energy of the CG at the critical plane. Inside the critical plane the speed of the CG is zero, therefore:

$$E_i = V_2 - V_1 - K_1 \tag{5}$$

The increment of potential energy, $V_2 - V_1$, is the sum of potential energy due to gravity, $\mathbf{F_G}$, and the rest of forces and moments, $\mathbf{F_{RI}}$ and $\mathbf{M_R}$, that is:

$$V_2 - V_1 = \Delta V_G + \Delta V_F + \Delta V_M \tag{6}$$

$$\Delta V_G = mgh \tag{7}$$

$$\Delta V_F = \int_{\theta_1}^{\theta_2} (\mathbf{F_{RI}} \times \mathbf{R}) \cdot \mathbf{e_i}\, d\theta \tag{8}$$

$$\Delta V_M = \int_{\theta_1}^{\theta_2} (\mathbf{M_R} \cdot \mathbf{e_i})\, d\theta \tag{9}$$

where vectors $\mathbf{R}$ and $\mathbf{e_i}$ are defined in Figure 1. Let us consider the speed of the CG before the tumble (1), $\mathbf{v}_{CG}$. The kinetic energy at that instant is obtained from the angular momentum:

$$L_i = (\mathbf{R} \times m\mathbf{v}_{CG}) \cdot \mathbf{e}_i \tag{10}$$

where m is the total mass of the robot and its manipulator system. Then the angular speed of the robot before the tumble comes from:

$$\omega_i = \frac{L_i}{I_i} \tag{11}$$

where I_i is the moment of inertia around the rotation axis. Thus the kinetic energy of the system before the tumble is:

$$K_1 = \frac{1}{2} I_i \omega_i^2 \tag{12}$$

The term E_i in equation (4) is the increment of mechanical energy of the CG when pivoting around the edge i of the support polygon. It is also the increment of the machine's stability level when the machine is rotating around that axis due to an impulsive perturbation. Therefore let us propose the following definition:

Definition 2.1 *A walking machine is dynamically stable if every momentum M_i around the i-edge of the support polygon due to robot/ground forces and moments is positive. A moment is positive if it goes around the support polygon in the clockwise direction.*

That is:

$$M_i > 0\,, i = 1..n-1 \tag{13}$$

where i is the edge of the support polygon, and n is the number of supporting feet. M_i is the moment around the axis i and comes from:

$$M_i = (\mathbf{F_R} \times \mathbf{R} + \mathbf{M_R}) \cdot \mathbf{e_i} \tag{14}$$

If equation (13) is true the robot is stable and then the **Normalized Dynamic Energy Stability Margin** is defined as:

Definition 2.2 *The* **Normalized Dynamic Energy Stability Margin, NDESM**, *is the smallest of the stability levels required to tumble the robot around the support polygon, normalized to the robot mass, that is:*

$$S_{MEEDN} = \frac{\min(E_i)}{mg} \tag{15}$$

where E_i is the stability level, given by (4).

The next section shows through simulation the improvement in stability margin measurement achieved using the proposed NDESM with different terrain profiles and dynamic effects.

3 Validation of the NDESM

After defining the NDESM, this section analyzes how walking-robot stability measurement is improved using the stability margin herein proposed. A comparison between the NDESM and other classic stability margins is performed through numerical simulation of a walking robot in the following scenarios:

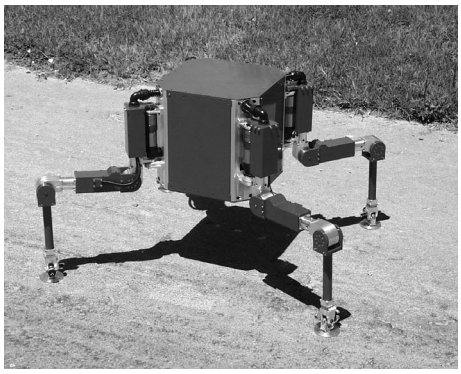

Figure 2: The SILO4 walking robot

- Under static conditions.
- On inclined ground and subject to inertial effects.
- On inclined ground and subject to inertial and manipulation effects.

A commercial Simulation Construction Set (SCS) [12] was chosen for this purpose because it provides suitable tools for dynamic simulation. The SILO4 quadruped robot [6], shown in Figure 2, was used as a comparative testbed, and the stability margins were computed while the robot was walking using a two-phase discontinuous gait [3]. Using the Java-based SCS library, robot kinematics and dynamics were defined as well as the ground profile and ground contact model.

Previous work on the classification of stability margins for walking machines [1] reveals that the FASM and the DSM (definitions of these stability margins are shown in the Appendix A) are the most suitable stability margins when the robot is subject to dynamic effects. Therefore, in this paper the proposed NDESM is compared with the FASM and the DSM. Figures 3 and 4 show numerical results, which are analyzed in the following subsections.

3.1 NDESM under static conditions

Under static conditions, the only force acting on the robot is gravity because $\mathbf{F_{RI}} = 0$ and $\mathbf{M_R} = 0$. Therefore the resultant robot/ground interaction force becomes:

$$\mathbf{F_R} = \mathbf{F_G} \tag{16}$$

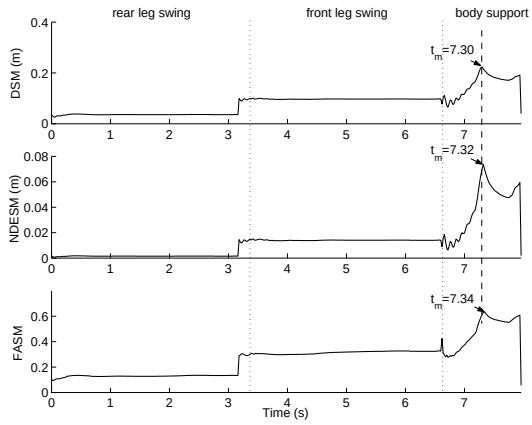

Figure 3: DSM, NDESM and FASM during half a gait cycle when inertial and elastic effects arise on terrain inclined 10^o from the horizontal plane.

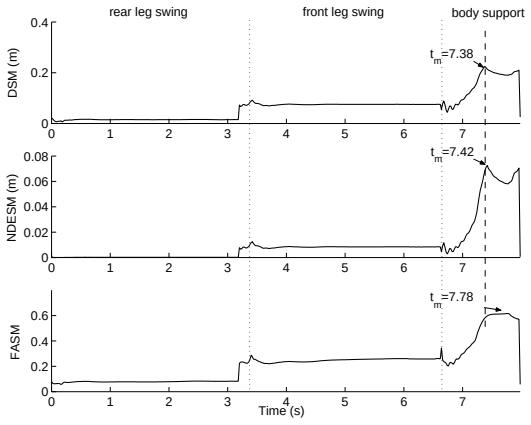

Figure 4: DSM, NDESM and FASM during half a gait cycle when inertial and elastic effects arise and a 20-N manipulation force opposes robot motion on terrain inclined 10^o from the horizontal plane.

Under such conditions, the critical plane coincides with the vertical plane, and the NDESM becomes:

$$S_{NDESM} = \min \frac{|\mathbf{R}|(1 - cos\theta)cos\psi}{mg} \qquad (17)$$

The above expression of the NDESM matches the definition of the NESM (see equation 20). Therefore, under static conditions the NDESM and the NESM coincide. In such conditions, the NESM has been proved to be optimum [5]; therefore the NDESM is optimum too.

3.2 NDESM subject to inertial and manipulation effects

When the walking robot is subject to inertial effects due to its own body motion and manipulation effects caused by leg-transfer motion or robot-manipulator tasks, the NESM fails to measure robot stability. However, as Figures 3 and 4 show, the NDESM is suitable for measuring robot stability under such conditions. The DSM, NDESM, and FASM are represented during half a gait cycle, which consists of the transfer of the rear leg, followed by the transfer of the adjacent front leg, and lastly body propulsion. Figure 3 compares the three stability margins when the terrain is inclined 10 degrees and there are inertial effects, and Figure 4 shows the effect of a 20-N manipulation force on the stability of a robot walking under the same terrain-inclination conditions. Joint elasticity has been also considered in the four scenarios.

These two figures show that the NDESM undergoes oscillations due to joint elasticity and reflects stability losses caused by inertia on the motion of the body and the legs during their transfer. The FASM and the DSM also undergo such modifications. However, when the robot is subject to manipulation forces the instant of maximum stability differs from one criterion to the other. In such a scenario the instant of maximum NDESM precedes the instant of maximum FASM and takes place after the instant of maximum DSM, as shown in Figures 3 and 4. These differences between the three stability margins persist for different terrain inclinations and manipulation forces. This is shown in Figures 5(a) and (b), where the instants of maximum DSM and FASM are compared with the instant of maximum NDESM for different terrain-inclination angles and different manipulation forces.

To determine which of the three stability margins is the best an unstable situation has been simulated and stability margins have been computed. A 25-N external force opposing the robot's motion was simulated and the robot tumbled down. Dimensionless stability margins have been computed in order to permit numerical comparison. For this purpose, the NDESM has been divided by the robot height ($H = 0.34$ m), and the DSM has been divided by half the stroke pitch ($P/2 = 0.5$ m). Figure 6(a) shows the three stability margins before and after the tumble occurs (at $t = 0.1$ s). After the tumble the three stability margins become zero. However, before the tumble, the three stability margins behave differently. The FASM reflects a delay in measuring the stability decrease just before the tumble, while the DSM and the NDESM show the stability decrease from the beginning of the motion.

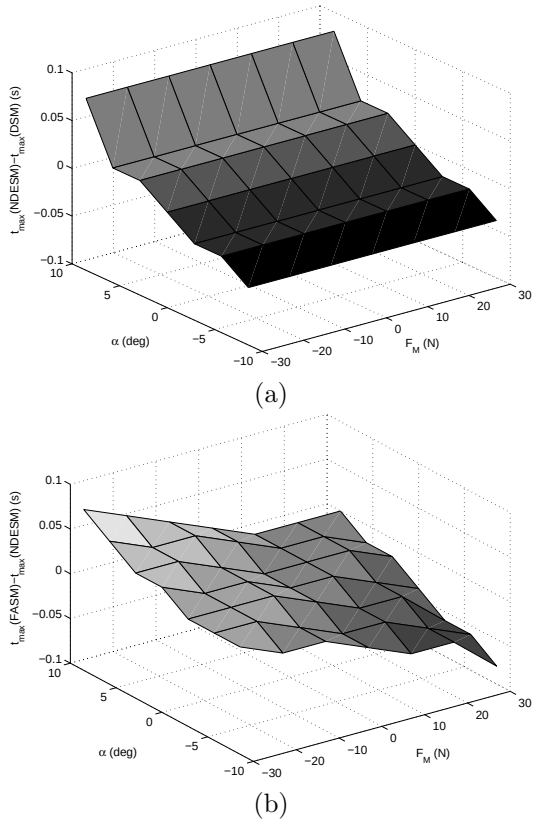

Figure 5: Difference between instants of maximum stability for several terrain inclinations (α) and manipulation forces (F_M). (a) DSM vs. NDESM. (b) FASM vs. NDESM.

Nevertheless, the DSM exhibits a discontinuity at the instant of tumble. This is clarified in Figure 6(b), where derivatives of the three stability margins are shown. An impulse on derivatives of the DSM and FASM reveals an error in the instability prediction. As Figures 6(a) and (b) show, the NDESM becomes zero continuously, and thus no prediction error exists. Therefore, the NDESM has no error in the measurement of robot stability and can be used to predict robot instability precisely.

4 Conclusions

Previous work on the analysis and classification of stability margins for walking machines has claimed that none of the existing stability margins have succeeded in measuring robot stability precisely when inertial and manipulation effects perturb the robot's motion. In this paper, a new stability margin named

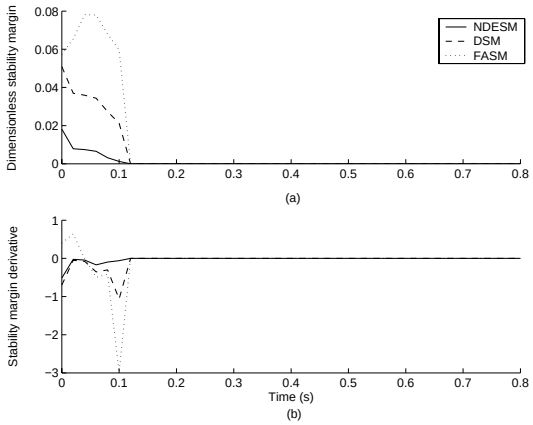

Figure 6: Unstable situation due to an external force of -25 N.(a) Dimensionless DSM, NDESM and FASM; (b) Dimensionless DSM, NDESM and FASM derivatives

NDESM has been proposed. The NDESM is an extension of the NESM to account for the presence of inertial and manipulation effects acting on the robot's CG. In this paper, it has been shown that the proposed NDESM is the only stability margin that provides a precise stability measurement in the presence of robot dynamics and manipulation effects.

Acknowledgments

The authors want to thank Jerry Pratt for his help using the simulation software package.

This work has been partially funded by CICYT (Spain) through Grant DPI2001-1595.

References

[1] E. Garcia, J. Estremera, and P. Gonzalez de Santos. A comparative study of stability margins for walking machines. *Robotica*, 20, 2002. In Press.

[2] A. Ghasempoor and N. Sepehri. A measure of stability for mobile manipulators with application to heavy-duty hydraulic machines. *ASME Journal of Dynamic Systems, Measurement and Control*, 120:360–370, 1998.

[3] P. Gonzalez de Santos and M.A. Jimenez. Generation of discontinuous gaits for quadruped walking machines. *Journal of Robotic Systems*, 12(9):599–611, 1995.

[4] P. Gonzalez de Santos, M.A. Jimenez, and M.A. Armada. Dynamic effects in statically stable walking machines. *Journal of Intelligent and Robotic Systems*, 23(1):71–85, 1998.

[5] S. Hirose, H. Tsukagoshi, and K. Yoneda. Normalized energy stability margin: Generalized stability criterion for walking vehicles. In *Proc. Int. Conf. Climbing and Walking Robots*, pages 71–76, November 1998. Brussels, Belgium.

[6] Industrial Automation Institute, C.S.I.C., Madrid, Spain. *The SILO4 Walking Robot*, 2002. Available: http://www.iai.csic.es/users/silo4/.

[7] B.S. Lin and S.M. Song. Dynamic modeling, stability and energy efficiency of a quadrupedal walking machine. In *Proc. IEEE Int. Conf. Robotics and Automation*, pages 367–373, 1993. Atlanta, Georgia.

[8] R.B. McGhee and A.A. Frank. On the stability properties of quadruped creeping gaits. *Mathematical Bioscience*, 3:331–351, 1968.

[9] D.A. Messuri. *Optimization of the locomotion of a legged vehicle with respect to maneuverability*. PhD thesis, The Ohio State University, 1985.

[10] E.G. Papadopoulos and D.A. Rey. A new measure of tipover stability margin for mobile manipulators. In *Proc. IEEE Int. Conf. Robotics and Automation*, pages 3111–3116, April 1996. Minneapolis, Minnesota.

[11] S.M. Song and K.J. Waldron. *Machines that walk: The adaptive suspension vehicle*. The MIT Press, Cambridge, Massachusetts, 1989.

[12] Yobotics Inc., Boston, MA. *Yobotics! Simulation Construction Set: Users Guide*, 2002. Available: http://www.yobotics.com/.

A Definition of Stability Margins

The stability margins that have been used for numerical comparison in Section 3 are herein defined.

A.1 Energy Stability Margin, ESM

Messuri [9] defined the ESM as the minimum potential energy required to tumble the robot around the edges of the support polygon, that is:

$$S_{ESM} = \min_{i}^{n_s}(mgh_i) \tag{18}$$

where i denotes the segment of the support polygon considered the rotation axis, n_s is the number of supporting legs, and h_i is the variation of CG height during the tumble, which comes from:

$$h_i = \mid \mathbf{R_i} \mid (1 - cos\theta)cos\psi \tag{19}$$

where R_i is the distance from the CG to the rotation axis, θ is the angle that R_i forms with the vertical plane, and ψ is the inclination angle of the rotation axis relative to the horizontal plane.

A.2 Normalized Energy Stability Margin, NESM

Hirose *et al.* normalized the ESM to the robot's weight and proposed the NESM, defined as [5]:

$$S_{NESM} = \frac{S_{ESM}}{mg} = \min_{i}^{n_s}(h_i) \tag{20}$$

A.3 Dynamic Stability Margin, DSM

Lin and Song [7] defined the DSM as the smallest of all moments M_i around the edges of the support polygon caused by robot/ground interaction forces, normalized by the weight of the system, that is:

$$S_{DSM} = min_i\left(\frac{M_i}{mg}\right) = min_i\left(\frac{\mathbf{e}_i \cdot (\mathbf{F}_R \times \mathbf{P}_i + \mathbf{M}_R)}{mg}\right) \tag{21}$$

where P_i is the position vector from the CG to the *i-th* support foot, F_R and M_R are the resultant force and moment of robot/ground interaction, and $\mathbf{e_i}$ is a unit vector that revolves around the support polygon in the clockwise sense.

A.4 Force-Angle Stability Margin, FASM

Proposed by Papadopoulos and Rey [10]. The Force-Angle stability criterion finds the angle α_i between the resultant force acting from the CG on the ground (the opposite to the reaction force F_R) and the vector R_i, normal to the rotation axis from the CG. The system becomes unstable when this angle becomes zero. The stability margin is the product of the angle times the resultant force F_R, that is:

$$S_{FASM} = min(\alpha_i) \cdot \|\mathbf{F}_R\| \tag{22}$$